

Annealing temperature dependence of local piezoelectric response of (Pb, Ca)TiO₃ ferroelectric thin films



R.A. Capeli^a, F.M. Pontes^{a,*}, A.J. Chiquito^c, W.B. Bastos^f, Marcelo A. Pereira-da-Silva^{d,e}, E. Longo^{b,f}

^a Department of Chemistry, Universidade Estadual Paulista - Unesp, P.O. Box 473, 17033-360 Bauru, São Paulo, Brazil

^b LIEC – Department of Chemistry, Universidade Federal de São Carlos, Via Washington Luiz, Km 235, P.O. Box 676, 13565-905 São Carlos, São Paulo, Brazil

^c NanO LaB – Department of Physics, Universidade Federal de São Carlos, Via Washington Luiz, Km 235, P.O. Box 676, 13565-905 São Carlos, São Paulo, Brazil

^d Institute of Physics of São Carlos, USP, São Carlos 13560-250, São Paulo, Brazil

^e UNICEP, São Carlos 13563-470, São Paulo, Brazil

^f Institute of Chemistry, Universidade Estadual Paulista – Unesp, Araraquara, São Paulo, Brazil

ARTICLE INFO

Keywords:

Chemical solution deposition

Thin films

Piezoresponse force microscopy

ABSTRACT

In this work, we have systematically investigated the piezo/ferroelectric response of (Pb, Ca)TiO₃ thin films prepared by polymeric precursor method using simultaneously topography, piezoresponse force microscopy (PFM) and local piezoelectric hysteresis loop measurements. The thin films were grown on Pt/Ti/SiO₂/Si substrates and annealed at 400, 500 and 600 °C and subjected to structural characterization using x-ray diffraction, infrared and micro-Raman spectroscopy. The ferroelectric domains structure and the piezoelectric response evolved as a function of thermal annealing temperature as well as the density of active grains (number of switchable domains) progressively increased. Another important characteristic of these films is the onset of large area showing the coexistence of active (stronger piezoresponse signal) and inactive (weak or non piezoresponse signal) grains embedded in the polycrystalline perovskite matrix. A combination of out-of-plane (OP) and in-plane (IP) PFM images revealed local features of polarization component magnitudes in samples surface. Well-defined local piezoelectric hysteresis loop was achieved on top of individual nanometer-scale grains in both samples annealed at 500 and 600 °C, and the switching behavior is evident.

1. Introduction

One of the important topics in perovskite-type ferroelectric materials technology is the knowledge the exact nature of the local piezoelectric and ferroelectric response [1,2]. Since characteristics such as size, shape, orientation, crystallization temperature, defects and doping level are recognized to modify piezo/ferroelectric properties, this topic has attracted much attention as an important issue in the nano-science field [3–6]. In particular, piezoresponse force microscopy (PFM) is a powerful tool for nanoscale investigation in piezo/ferroelectric materials. For example, the size effect indicates the disappearance of ferroelectricity in perovskite-type ferroelectric of dimensions smaller than a critical value [7]. In addition, the influence of doping type on the formation of ferroelectric perovskite materials showed that iron doping induces the disappearance of ferroelectricity in (Pb,Sr)(Ti,Fe)O₃ thin films [8]. Puli et al. [9] observed a strong domain switching response at

nanoscale level by using PFM in (Ba_{0.50}Sr_{0.50})(Ti_{0.80}Sn_{0.20})O₃ thin films a. Furthermore, Huang et al. [10] reported PFM images in which domain boundaries are in agreement with grain boundaries in Bi_{3.15}Nd_{0.85}Ti₃O₁₂ ferroelectric thin films, suggesting that grain boundaries entirely confine the shape of domain boundaries. In Bi_{0.70}A_{0.30}FeO₃ (A=Ca, Sr, Pb and Ba) ceramic solid solution, Khomchenko et al. [11] investigated the relationship connecting piezo/ferroelectric responses and the presence of A-site dopants. They observed a reduction of the polarization due to the presence of A-site dopants which was confirmed by piezoresponse force microscopy data. Recently, piezoresponse force microscopy studies revealed an intense local polarization response in the out-of-plane direction in multi-layered structures consisting of single Ba(Zr_{0.10}Ti_{0.90})O₃ and (Ba_{0.75}Ca_{0.25})TiO₃ layers fabricated on Nb doped (001) SrTiO₃ (Nb:STO) substrates by pulsed laser deposition [12].

In this paper, we used piezoresponse force microscopy to observe

* Corresponding author.

E-mail address: fenelon@fc.unesp.br (F.M. Pontes).

<http://dx.doi.org/10.1016/j.ceramint.2017.01.015>

Received 1 April 2016; Received in revised form 4 January 2017; Accepted 4 January 2017

Available online 05 January 2017

0272-8842/ © 2017 Elsevier Ltd and Techna Group S.r.l. All rights reserved.

crystallization temperature effects on local of piezo/ferroelectric properties of chemical solution deposition (CSD) prepared (Pb, Ca)TiO₃ thin films.

2. Experimental procedures

Our procedure for synthesizing (Pb_{0.74}Ca_{0.26})TiO₃ thin films consisted in producing a polymeric resin using a soft chemistry method (polymeric precursor route). Specific details of this synthesis is found in the literature [13]. Pt/Ti/SiO₂/Si wafers were used as substrates. The substrate was spin-coated by dropping a small amount of the precursor solution. The rotation speed and the spin time were fixed at 5000 rpm and 30 s, respectively, to ensure that the film thickness was uniform on the substrate. Each layer was dried at 150 °C after the spin coating on a hot plate for 30 min to remove residual solvents. After the pre-annealing, the films were annealed at 400, 500 and 600 °C for 2 h in air atmosphere. In addition, thicknesses of 370 nm, 315 nm, and 330 nm were obtained at 400, 500 and 600 °C, respectively.

(Pb_{0.74}Ca_{0.26})TiO₃ thin films were then structurally characterized by XRD in the θ - 2θ scan mode (steps of 0.02°) which was recorded on a Rigaku MiniFlex600 diffractometer. Raman measurements were taken

with a T-64000 Jobin-Yvon triple-monochromator coupled to a charge-coupled device (CCD) detector. An optical microscope with a 100x objective was used to focus the 514.5 nm line of the Coherent Innova 90 Argon laser onto the sample; the power was maintained at 15 mW. Infrared analyses were performed using an Equinox/55 (Bruker) Fourier transformed infrared (FTIR) spectrometer to observe variations in chemical bond densities as a function temperature crystallization. FTIR reflectance spectra were recorded at room temperature from 350 to 1200 cm⁻¹ using a 30° specular reflectance accessory.

The topography, the polarization pattern of ferroelectric domain structures and the local hysteresis loops were investigated at the nanoscale level on ferroelectric thin films using a commercial AFM (MultiMode Nanoscope V, Bruker) modified to be used as a piezo-response force microscopy (PFM). The system was equipped with a lock-in amplifier (SR850, Stanford) and a function generator (33220 A, Agilent). During all PFM measurements, the conductive probe ($k=42$ N/m) was electrically grounded and an external voltage was applied to the bottom Pt electrode operated with a driving amplitude of 1 V (rms). The piezoresponse signal was recorded in PR = A*Cos(φ), and the piezoloops were obtained in the remnant mode.

In addition, a ferroelectric tester workstation (Radiant

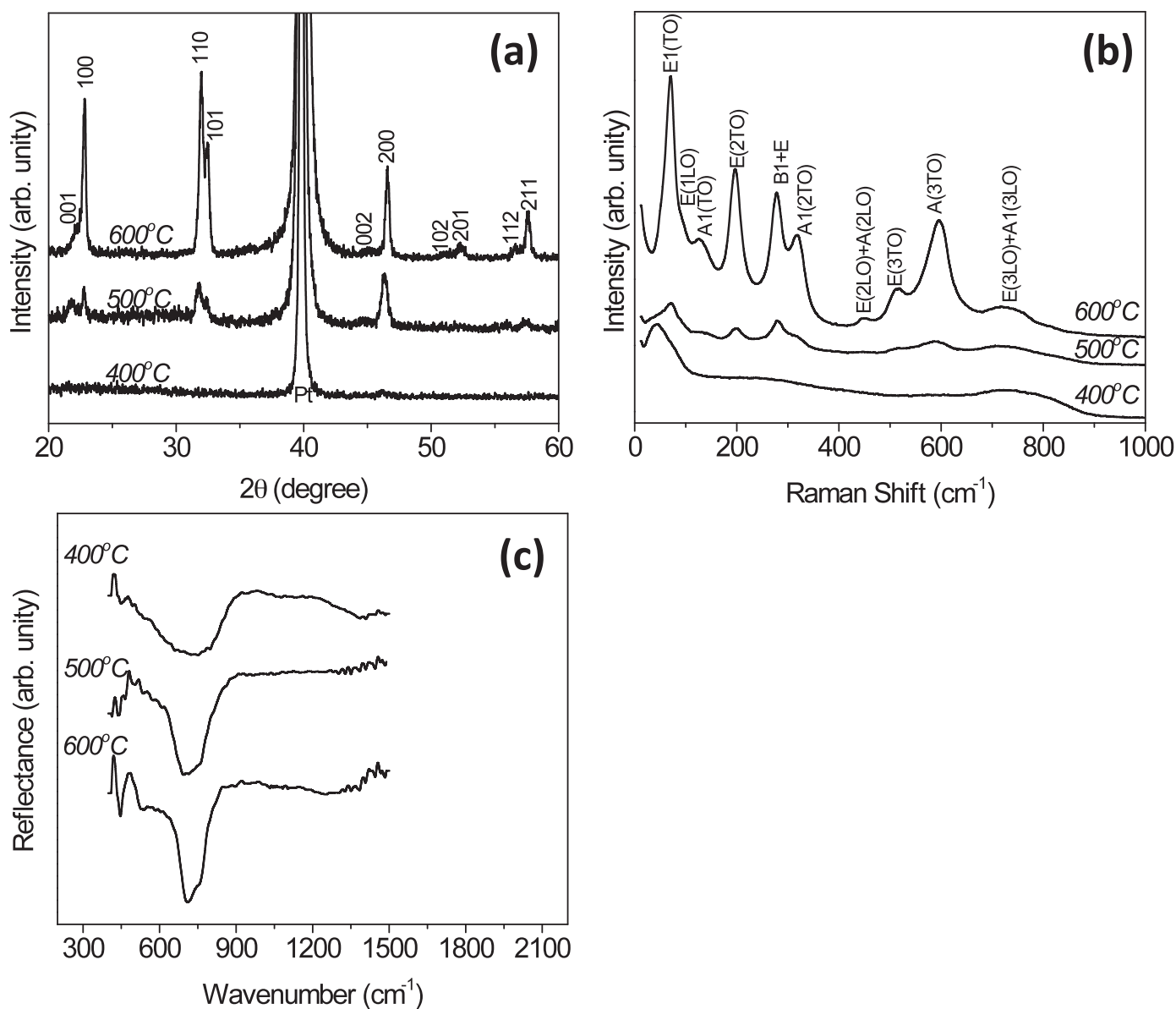


Fig. 1. (a) XRD patterns, (b) micro-Raman spectra and (c) FTIR spectra of Pb_{0.76}Ca_{0.24}TiO₃ thin films annealed at different temperatures.

Technologies, model Precision Premier II) was employed to study the ferroelectric behaviors of the thin films at the macroscopy level. For these measurements, circular gold electrodes of $4.9 \times 10^{-2} \text{ mm}^2$ used as top electrodes were deposited (using a shadow mask) by thermal evaporation (Edwards, model HHV AUTO306) on films surfaces.

3. Results and discussions

Fig. 1(a) shows XRD patterns of $(\text{Pb}_{0.74}\text{Ca}_{0.26})\text{TiO}_3$ thin films deposited on Si/SiO₂/Ti/Pt substrates after calcination at several temperatures. A diffuse X-ray diffraction (XRD) pattern was observed at 400 °C, indicating the formation of an amorphous phase. At 500 °C, crystallization of $(\text{Pb}_{0.74}\text{Ca}_{0.26})\text{TiO}_3$ phase was observed. Generally, higher annealing temperatures will result in a better crystalline quality. As the annealing temperature increased to 600 °C, the relative intensity of the XRD patterns of thin films increased as well. The higher relative XRD intensity can indicate an improved crystallinity, an increase of grain sizes and the presence of reduced amounts of the amorphous phase. The splitting of the peaks at 2θ of (001)/(100) and (110)/(101) was clearly observed meaning that at 500 °C these films begin to crystallize in the tetragonal perovskite phase [14].

The Raman spectra of the $(\text{Pb}_{0.74}\text{Ca}_{0.26})\text{TiO}_3$ thin films are shown in Fig. 1(b). Typical Raman modes for tetragonal structure [15] are observed for temperatures above 400 °C. In a close agreement with the XRD results, the films exhibit an amorphous structural phase after an annealing at 400 °C: a broad shoulder was observed between 150–350 and 650–900 cm^{-1} . Increasing the temperature, the intensities of the Raman peaks increase as well showing an improvement of the films crystalline quality.

The results of FTIR show that the films are crystallized when using annealing temperatures above 400 °C, as already observed by XRD and micro-Raman results. From the FTIR results shown in Fig. 1(c), it is observed a broader absorption peak between 600 and 840 cm^{-1} at 400 °C suggesting the formation of an amorphous structural phase.

After annealing at 500 and 600 °C, the films exhibited well-defined absorption peaks, between 600 and 840 cm^{-1} , due to a better short-range structural ordering and a consequent increase in films crystallinity. Similar observation was already reported in literature [16].

Fig. 2(a–f) show the piezoresponse force microscopy (PFM) images, (simultaneously obtained with the topography images) of $(\text{Pb}_{0.74}\text{Ca}_{0.26})\text{TiO}_3$ films after annealing at 400, 500 and 600 °C. From topography images depicted in Fig. 2(a), one observed that after annealing at 400 °C, $(\text{Pb}_{0.74}\text{Ca}_{0.26})\text{TiO}_3$ films did not shown any apparent grain growth. As a result, the out-of-plane PFM images of films at 400 °C showed absence of contrast; therefore, there was no piezoresponse signal as depicted in Fig. 2(d). After an annealing at 500 °C, topography analysis revealed partial growth of grains (Fig. 2(b)). These images clearly show that the grain growth occurs in the surrounding amorphous matrix. Fig. 2(e) displays the piezoresponse image of films annealed at 500 °C. The dark and bright contrast of piezoresponse image indicate that the domain structures are present in thin films. Here, in the out-of-plane PFM image, light contrast corresponds to the vertical component of polarization pointing upward (in our case, positive polarization), whereas dark contrast corresponds to the vertical component of polarization pointing downward (in our case, negative polarization) and intermediate contrast near the center of the scale bar corresponds polarization pointing at any direction in plane of surface or non-polarization. A striking feature of the PFM image in Fig. 2(e) is the presence of intermediate color (between the center of the scale bar and end scale: dark or light); this indicates that the vertical component of the polarization distribution of the grains is random (solid blue arrow). Another interesting feature is the presence of a flat background between grains (solid yellow arrow), showing a uniform color. These results demonstrate zero spontaneous polarization (not exhibiting piezoelectric effect). After annealing at 600 °C, $(\text{Pb}_{0.74}\text{Ca}_{0.26})\text{TiO}_3$ films topography showed densely packed grains due to grains growth, reduced amounts of amorphous phase, distinct grain boundaries, uniform grains and better crystallization as shown in

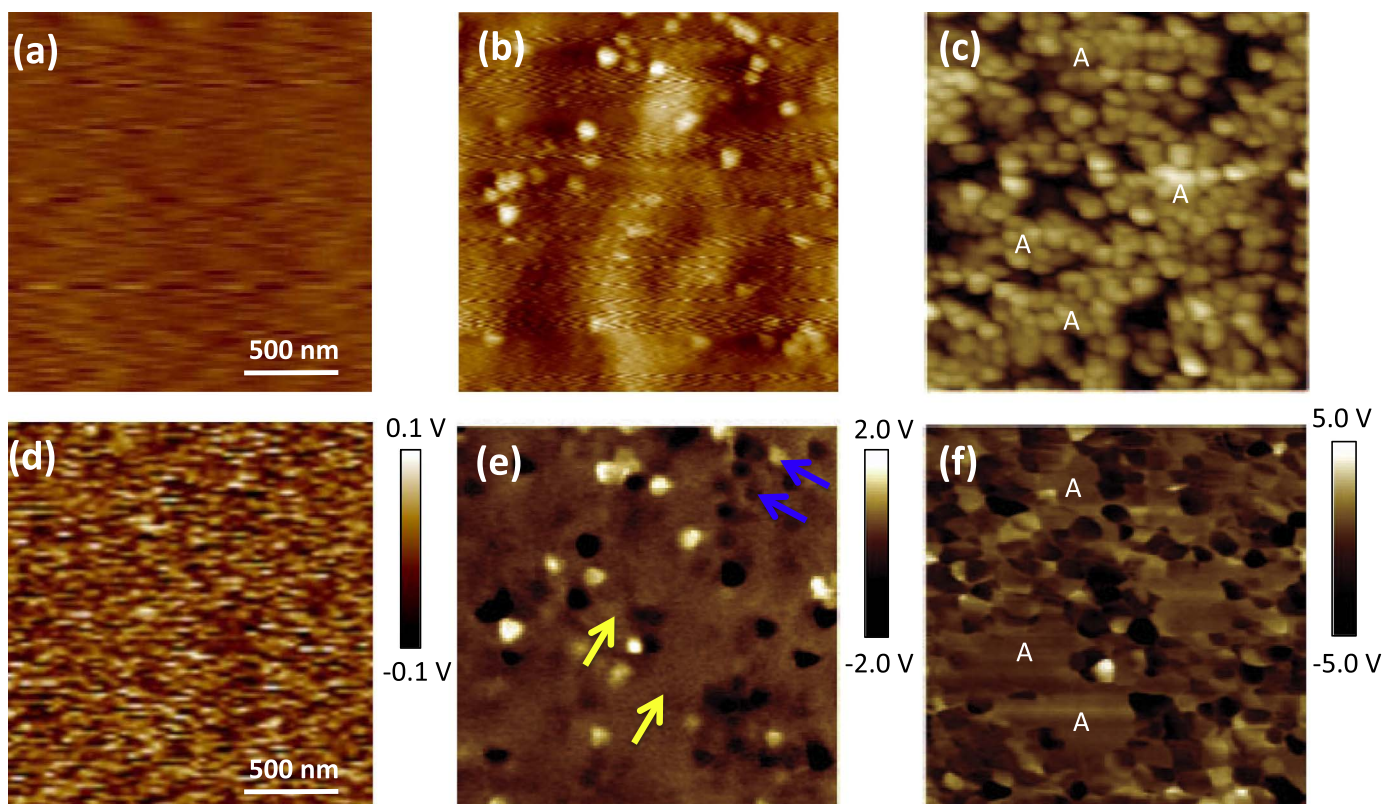


Fig. 2. (a–c) Topography and (d–f) domains structures, out-of-plane PFM images of $\text{Pb}_{0.76}\text{Ca}_{0.24}\text{TiO}_3$ thin films annealed at (a) 400, (b) 500 and (c) 600 °C. ($2 \times 2 \mu\text{m}^2$ scan). (For interpretation of the references to color in this figure legend, the reader is referred to the web version of this article).

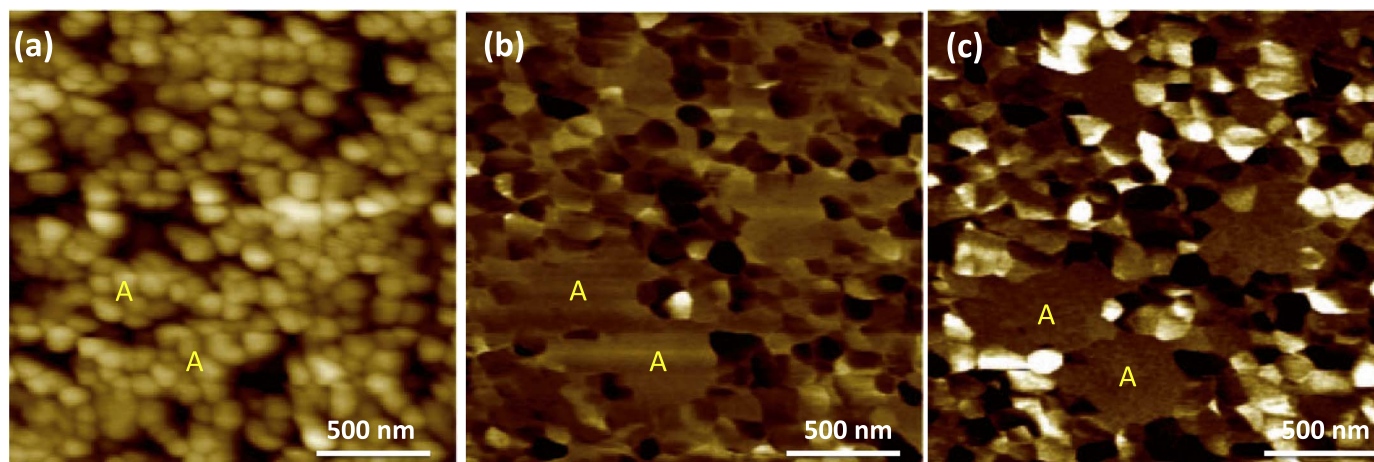


Fig. 3. (a) Topography image ($2 \times 2 \mu\text{m}^2$ scan), (b) out-of-plane PFM image, and (c) in-plane PFM image ($2 \times 2 \mu\text{m}^2$ scan), simultaneously recorded on $\text{Pb}_{0.76}\text{Ca}_{0.24}\text{TiO}_3$ thin films annealed at 600°C . Regions labeled A represent grain groups without piezoresponse signal (inactive grains).

Fig. 2(c). This is consistent with results reported by Kartawidjaja et al. [17]. All these features support the XRD, micro-Raman and FTIR data and above discussions. As a result, out-of-plane PFM images of films annealed at 600°C show well-contrasted piezoresponse patterns (Fig. 2(f)). In PFM image, different colors (bright, light brown, dark brown and black) represent different orientation of local polarization. Therefore, these images clearly reveal that polarization orientation distribution is arbitrarily and randomly distributed over the whole polycrystalline thin film. In addition, a flat background can be distinguished in the out-of-plane PFM image (labeled A). This can be understood in the following way: in some regions, groups of nanometer grains seem to behave as if they were inactive (weak or non piezoelectric activity), shown in both topography/PFM images (labeled A). In order to investigate if these regions (labeled A) have an in-plane polarization component, in-plane PFM images were taken. Therefore, combinations of out-of-plane and in-plane PFM images provide information about the polarization orientation [18] along the z-axis and y-axis, respectively, as shown in Fig. 3. Important observations can be made regarding the in-plane PFM image: first the majority of grains exhibit both white (positive) and dark (negative) contrast in-plane (piezoelectric activity), highlighting the non-existence of a preferred polarization direction at the nanometer scale in-plane direction. This result indicates the arbitrary polarization orientation over the whole polycrystalline thin film. Fig. 3(c) was recorded in exactly same area with respect to out-of-plane PFM image; second, the in-plane PFM image (Fig. 3(c)) shows the same flat profile background (no piezoresponse signal) with respect to out-of-plane PFM image, taken in the same area scans (labeled A). Considering the out-of-plane and in-plane PFM images as discussed above, there are strong evidences of non-ferroelectric nature of these groups of grains, i.e., without showing out-of-plane and in-plane polarization components. A similar analysis of the presence inactive groups grains (non-piezo/ferroelectric activity) surrounding active groups grains matrix (piezo/ferroelectric activity) in crystalline materials was reported by other authors [19–21].

In order to locally investigate the polarization switching quality of films, a dc bias was applied to the conducting AFM tip probe while scanning over the desired area (Fig. 4). Local poling “writing” was achieved on a square-shaped area by applying alternately a dc voltage of $+12\text{ V}$ (white contrast) and -12 V (black contrast) to the conductive AFM tip, corresponding upward and downward polarization, respectively. For films annealed at 400°C the domain switching cannot be observed for the out-of-plane PFM image after applying the poling voltage of $\pm 12\text{ V}_{\text{bias}}$ (not shown here). The absence of switchable polarization effects demonstrates lack of short- and long-range ferroelectric domains ordering of amorphous phase. The out-of-plane PFM image acquired after poling in films annealed at 500°C clearly shows a

$2 \times 2 \mu\text{m}^2$ area that had been previously poled at its center with both positive (white contrast) and negative (dark contrast) bias, confirming the thin film switching, i.e., reverse behavior of ferroelectric polarization [Fig. 4(c)]. In addition, we observed regions (marked by solid blue arrow) which exhibit no contrast change; we can infer that these regions have no either piezoelectric nor ferroelectric activity (although the thin film have a certain tetragonality degree as indicated by the XRD and micro-Raman measurements). For films annealed at 600°C , local polarization switching is successfully performed, as evidenced by high contrast (dark and white contrast, corresponding to the two polarization states downward and upward, respectively) obtained after write/read operation (Fig. 4(d)). In this image, it can also be seen that a decrease in the area occupied by non switchable domains (grains) is consistent with the annealing temperature at 600°C which in turn, indicates better crystalline quality of grains. Furthermore, a careful observation shows that any domains (grains) was not switched completely with respect to the average surrounding grains after poling process. Similar observation has been observed in BiFeO_3 thin films prepared by sputtering [22]. Typical domains structure dispersion effects are usually ascribed as freezing short-range ferroelectric order (domains wall structure) [23,24]. In this way, the problem of inhomogeneous domains structure in nanoscale level will be reflected in the macroscopic electrical properties.

Fig. 5 shows the typical piezohysteresis obtained of selected individual grain using PFM experiments. The piezoelectric hysteresis loop gives information on the evolution of the ferroelectric domains structure as a function of annealing temperature.

As a first observation, well-defined piezohysteresis loop is clearly obtained from the PFM measurements recorded in the “remnant” mode at $+15\text{ V}$ dc voltages in both films annealed at 600°C and 500°C . However, we can also note that the local piezohysteresis response is higher in films annealed at 600°C than those at 500°C . In literature is reported that the magnitude of the piezohysteresis response depends on many factors, such as different crystallographic orientations of the grains, stress, crystallinity degree of grains, in-grain defects structure (vacancy, dislocation, impurities), grains shape and size (domains) [25–32]. As it is evident, the high crystallinity degree grains at 600°C (suggesting short- and long-range ferroelectric ordered domains structure) and relatively low crystallinity degree grains at 500°C (suggesting short- and long-range ferroelectric disordered domains structure) can be used to explain the variation in magnitude of the piezohysteresis loops response. In comparison, results for films annealed at 400°C , probe the existence of a non-switchable polarization (hysteresis loop is linear, indicative of non-ferroelectric nature).

Finally, Fig. 6 shown macroscopic ferroelectric hysteresis loops for thin films annealed at 400 , 500 and 600°C . The results obtained for

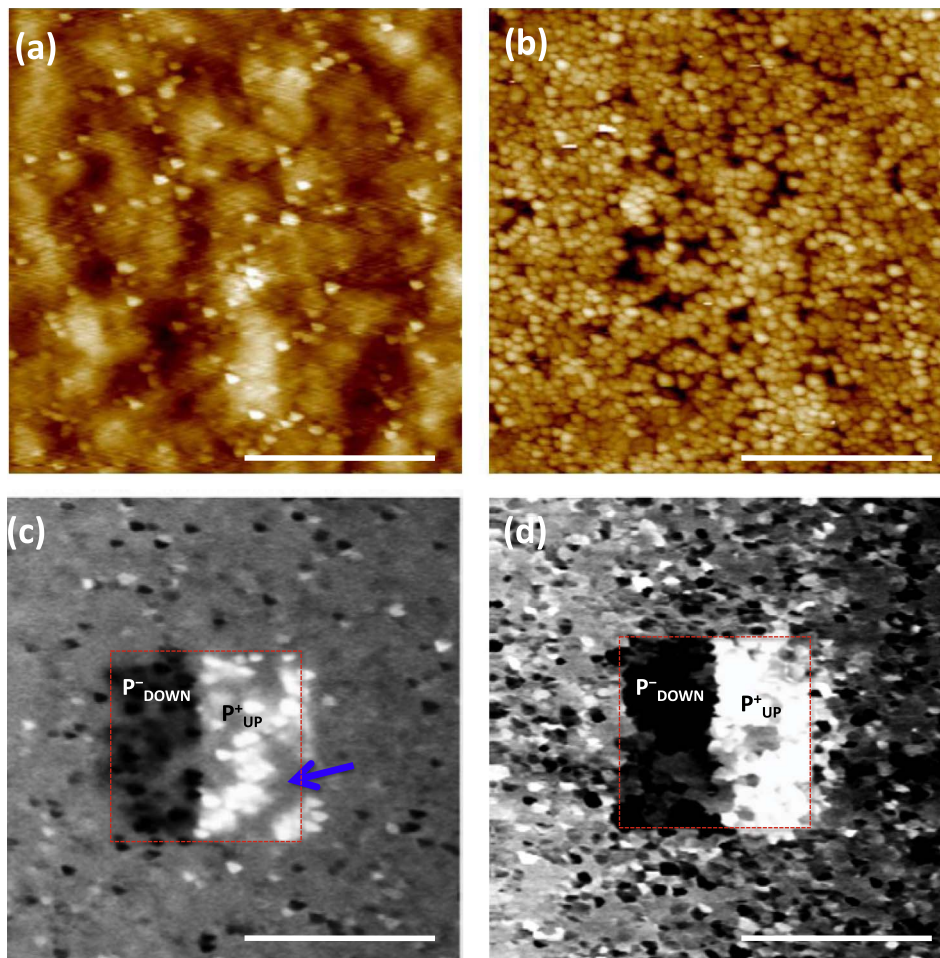


Fig. 4. Topography (a,b) and Out-of-plane PFM images after square-shape ($2 \times 2 \mu\text{m}^2$ scan) poling (external biases $\pm 12 \text{ V}$) of an arbitrary region in thin films annealed at 500 (a–c) and 600 °C (b–d). The scale bar is 2 μm . (For interpretation of the references to color in this figure, the reader is referred to the web version of this article).

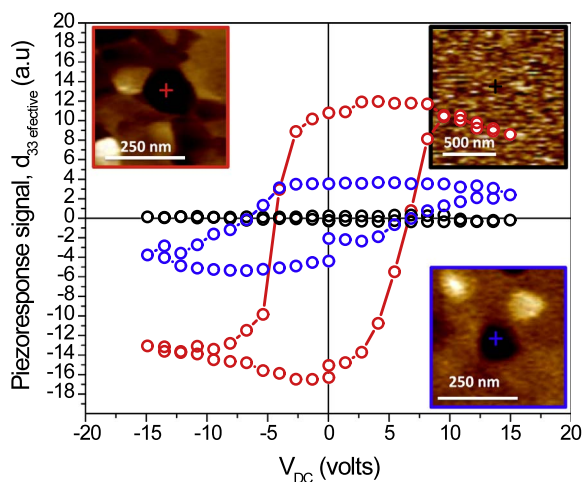


Fig. 5. Local Piezoelectric hysteresis loops acquired at the center of the grain indicated by symbol+(inset). Black, Blue and Red colors represent the thermal annealing temperature for $\text{Pb}_{0.76}\text{Ca}_{0.24}\text{TiO}_3$ films grown at 400, 500 and 600 °C, respectively. (For interpretation of the references to color in this figure legend, the reader is referred to the web version of this article).

films annealed at 400 °C show a linear behavior for hysteresis loop, i.e., non-ferroelectric nature. From Fig. 6, it can be seen a narrow and unsaturated ferroelectric hysteresis loop for films growth at 500 °C, characteristic of weak ferroelectricity. As a remark, we note a broad and well-saturated piezoelectric hysteresis loop taken on one grain (do-

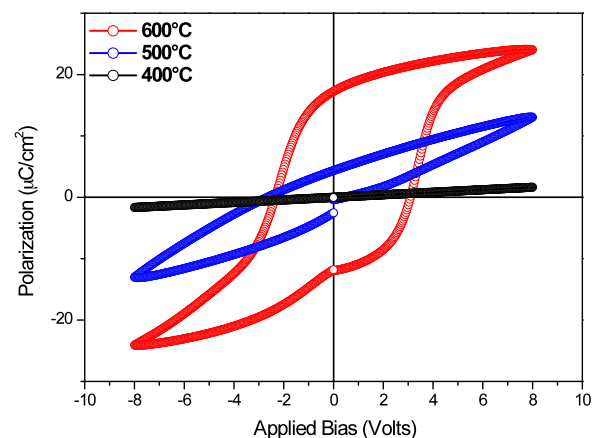


Fig. 6. Macroscopic ferroelectric hysteresis loops of (Pb, Ca) TiO_3 thin films grown at 400, 500 and 600 °C.

main) by PFM measurements for these films (see Fig. 5). It is true that the macroscopic ferroelectric hysteresis loop is measured for a wide group of grains (active and/or inactive grains) in a selected area on the thin films surface. For the films grown at 500 °C by polymeric precursor method, out-of-plane PFM images reveal large areas without piezoresponse signal. Therefore, macroscopically, the result is an average on only switching grains of each domain (active grains). On the other hand, the macroscopic result obtained for films grown at 600 °C showed a well-defined and saturated ferroelectric hysteresis

loop with remanent polarization value of $16 \mu\text{C}/\text{cm}^2$. These results are in very good agreement with piezoelectric hysteresis loop response in nanoscale level using PFM experiments.

4. Conclusions

In summary, we investigated the evolving of piezo/ferroelectric domain structures in $(\text{Pb}_{0.74}\text{Ca}_{0.26})\text{TiO}_3$ thin films grown by polymeric precursor method on Pt/Ti/SiO₂/Si substrate and the effects of thermal annealing at nanoscale level by PFM technique. XRD, FTIR and micro-Raman measurements confirm tetragonal crystalline structure of the thin films annealed at 500 and 600 °C. Clear domain structure, domain switching and measurable piezoresponse signal were observed in nanoscale level for films annealed at 500 and 600 °C. It was found by topography and PFM images that the domains structure is limited by grains sizes. It is worth noting that the maximum magnitude of piezoresponse signal was obtained for samples at 600 °C and is possibly due to improved crystallinity of the grains. Typical local well-defined piezoelectric hysteresis loop confirmed polarization switching on individual nanometer-scale grains. In particular, the out-of-plane and in-plane PFM images showed non-switchable regions occupied by nanometer-scale grains. An increase in the regions occupied by non-switchable grains and/or without piezoresponse signal is consistent with macroscopic ferroelectric hysteresis loop for films growth at 500 °C. Moreover we could observe by write/read operations that some grains (domains) apparently are opposite to positive and negative bias. This effect is attributed to domain wall pinning, or in other words, the domain wall movement is restricted.

Acknowledgments

This work was financially supported by the Brazilian agencies FAPESP and CNPq. We thank CEPID/CDMF/INCTMN. FAPESP process nos. 08/57150-6, 11/20536-7, 12/14106-2 and 13/07296-2. INCTMN process no. 08/57872-1. CNPq process nos. 573636/2008-7 and 470147/2012-1.

References

- B.J. Rodriguez, A. Gruverman, A.I. Kington, R.J. Nemanich, J.S. Cross, Investigation of the mechanism of polarization switching in ferroelectric capacitors by three-dimensional piezoresponse force microscopy, *Appl. Phys. A: Mater. Sci. Process.* 80 (2005) 99–103.
- N. Balke, Igor Bdkin, S.V. Kalinin, A.L. Kholkin, Electromechanical imaging and spectroscopy of ferroelectric and piezoelectric materials: state of the art and prospects for the future, *J. Am. Ceram. Soc.* 92 (2009) 1629–1647.
- Y.Q. Chen, Y.F. En, Y. Huang, X.D. Kong, X.J. Zheng, Y.D. Lu, Effects of surface tension and axis stress on piezoelectric behaviors of ferroelectric nanowires, *Appl. Phys. Lett.* 99 (2011) (203106-203106-3).
- P. Gao, C.T. Nelson, J.R. Jokisaari, Seung-Hyub Baek, C.W. Bark, Y. Zhang, E. Wang, D.G. Schlom, Chang-Beom Eom, X. Pan, Revealing the role of defects in ferroelectric switching with atomic resolution, *Nat. Commun.* 2 (591) (2011) 1–6.
- J.H. Lee, R.H. Shin, W. Jo, Polarization switching and relaxation dynamics of bismuth layered ferroelectric thin films: role of oxygen defect sites and crystallinity, *Phys. Rev. B* 84 (2011) (094112-094112-10).
- P. Khaenamkaew, S. Muensit, I.K. Bdkin, A.L. Kholkin, Effect of Zr/Ti ratio on the microstructure and ferroelectric properties of lead zirconate titanate thin films, *Mater. Chem. Phys.* 102 (2007) 159–164.
- A. Rudiger, T. Schneller, A. Roelofs, S. Tiedke, T. Schmitz, R. Waser, Nanosize ferroelectric oxides – tracking down the superparaelectric limit, *Appl. Phys. A* 80 (2005) 1247–1255.
- F.M. Pontes, D.S.L. Pontes, A.J. Chiquito, Marcelo A. Pereira-da-Silva, E. Longo, Effect of Fe-doping on the structural, microstructural, optical, and ferroelectric properties of $\text{Pb}_{1/2}\text{Sr}_{1/2}\text{Ti}_{1-x}\text{Fe}_x\text{O}_3$ oxide prepared by spin coating technique, *Mater. Lett.* 138 (2015) 179–183.
- V.S. Puli, S. Adireddy, D.K. Pradhan, R.S. Katiyar, D.B. Chrisey, Nanoscale ferroelectric switchable polarization and leakage current behavior in $(\text{Ba}_{0.50}\text{Sr}_{0.50})\text{TiO}_3$ thin films prepared using chemical solution deposition, *J. Nanomater.* 2015 (2015) 1–7.
- H. Huang, X.L. Zhong, S.H. Xie, Y. Zhang, J.B. Wang, Y.C. Zhou, Piezoresponse force microscopy observation of domain switching in $\text{Bi}_{3.15}\text{Nd}_{0.85}\text{Ti}_3\text{O}_{12}$ thin film prepared by pulsed laser deposition, *J. Appl. Phys.* 110 (2011) (054105-054105-4).
- V.A. Khomchenko, D.A. Kiselev, J.M. Vieira, Li Jian, A.L. Kholkin, A.M.L. Lopes, Y.G. Pogorelov, J.P. Araujo, M. Maglione, Effect of diamagnetic Ca, Sr, Pb, and Ba substitution on the crystal structure and multiferroic properties of the BiFeO_3 perovskite, *J. Appl. Phys.* 103 (2008) (024105-024105-6).
- X.N. Zhu, X. Xu, Z. Harrell, R. Guo, A.S. Bhalla, M. Zhang, J. Jiang, C. Chen, X.M. Chen, Ferroelectric domain structure evolution in $\text{Ba}(\text{Zr}_{0.1}\text{Ti}_{0.9})\text{O}_3/(\text{Ba}_{0.75}\text{Ca}_{0.25})\text{TiO}_3$ heterostructures, *RSC Adv.* 5 (2015) 65811–65817.
- D.S.L. Pontes, F.M. Pontes, R.A. Capeli, M.L. Garzim, A.J. Chiquito, E. Longo, Structural, ferroelectric, and optical properties of $\text{Pb}_{0.60}\text{Ca}_{0.20}\text{Sr}_{0.20}\text{TiO}_3$, $\text{Pb}_{0.50}\text{Ca}_{0.25}\text{Sr}_{0.25}\text{TiO}_3$ and $\text{Pb}_{0.40}\text{Ca}_{0.30}\text{Sr}_{0.30}\text{TiO}_3$ thin films prepared by the chemical solution deposition technique, *Ceram. Int.* 40 (2014) 13363–13370.
- I. Bretos, J. Ricote, R. Jiménez, J. Mendiola, R.J. Jiménez Riobóo, M.L. Calzada, Crystallisation of $\text{Pb}_{1-x}\text{Ca}_x\text{TiO}_3$ ferroelectric thin films as a function of the Ca^{2+} content, *J. Eur. Ceram. Soc.* 25 (2005) 2325–2329.
- F.M. Pontes, D.S.L. Pontes, E.R. Leite, E. Longo, A.J. Chiquito, P.S. Pizani, J.A. Varela, Electrical conduction mechanism and phase transition studies using dielectric properties and Raman spectroscopy in ferroelectric $\text{Pb}_{0.76}\text{Ca}_{0.24}\text{TiO}_3$ thin films, *J. Appl. Phys.* 94 (2003) 7256–7260.
- F.M. Pontes, E.R. Leite, M.S.J. Nunes, D.S.L. Pontes, E. Longo, R. Magnani, P.S. Pizani, J.A. Varela, Preparation of $\text{Pb}(\text{Zr,Ti})\text{O}_3$ thin films by soft chemical route, *J. Eur. Ceram. Soc.* 24 (2004) 2969–2976.
- F.C. Kartawidjaja, A. Varatharajan, N. Valanoor, J. Wang, Microstructure and texture development in single layered and heterolayered PZT thin films, *J. Mater. Sci.* 45 (2010) 6187–6199.
- C. Harnagea, M. Azodi, R. Nechache, C.-V. Cococar, V. Buscaglia, M.T. Buscaglia, P. Nanni, F. Rosei, A. Pignolet, Characterization of individual multifunctional nanoobjects with restricted geometry, *Phase Transit.* 86 (2013) 635–650.
- S. Gupta, A. Garg, D.C. Agrawal, S. Bhattacharjee, D. Pandey, Structural changes and ferroelectric properties of BiFeO_3 - PbTiO_3 thin films grown via a chemical multilayer deposition method, *J. Appl. Phys.* 105 (2009) (014101-014101-5).
- J. Ricote, G. Leclerc, D. Chateigner, P. Ramos, R. Bouregba, G. Poullain, Local piezoelectric properties of oriented PZT based ferroelectric thin films, *Ferroelectrics* 335 (2006) 191–199.
- S.V. Kalinin, R. Shao, D.A. Bonnell, Local phenomena in oxides by advanced scanning probe microscopy, *J. Am. Ceram. Soc.* 88 (2005) 1077–1098.
- J.W. Park, S.H. Baek, P. Wu, B. Winchester, C.T. Nelson, X.Q. Pan, L.Q. Chen, T. Tybell, C.B. Eom, Origin of suppressed polarization in BiFeO_3 films, *Appl. Phys. Lett.* 97 (2010) (212904-212904-3).
- A.Z. Simões, M.P. Cruz, A. Ries, E. Longo, J.A. Varela, R. Ramesh, Ferroelectric and piezoelectric properties of bismuth titanate thin films grown on different bottom electrodes by soft chemical solution and microwave annealing, *Mater. Res. Bull.* 42 (2007) 975–981.
- R.L. Gao, H.W. Yang, Y.S. Chen, J.R. Sun, Y.G. Zhao, B.G. Shen, Oxygen vacancies induced switchable and nonswitchable photovoltaic effects in $\text{Ag}/\text{Bi}_{0.9}\text{La}_{0.1}\text{FeO}_3/\text{La}_{0.7}\text{Sr}_{0.3}\text{MnO}_3$ sandwiched capacitors, *Appl. Phys. Lett.* 104 (2014) (031906-031906-5).
- A. Gruverman, A. Kholkin, Nanoscale ferroelectrics: processing, characterization and future trends, *Rep. Prog. Phys.* 69 (2006) 2443–2474.
- P. Khaenamkaew, I.K. Bdkin, A.L. Kholkin, S. Muensit, Local piezoresponse and ferroelectric domain of sol-gel $\text{Pb}(\text{Zr}_x\text{Ti}_{1-x})\text{O}_3$ film, *Songklanakarin J. Sci. Technol.* 30 (2008) 59–63.
- A.Z. Simões, B.D. Stojanovica, M.A. Ramirez, A.A. Cavaleiro, E. Longo, J.A. Varela, Lanthanum-doped $\text{Bi}_4\text{Ti}_3\text{O}_{12}$ prepared by the soft chemical method: rietveld analysis and piezoelectric properties, *Ceram. Int.* 34 (2008) 257–261.
- I. Coondoo, N. Panwar, H. Amorn, M. Alguero, A.L. Kholkin, Synthesis and characterization of lead-free $0.5\text{Ba}(\text{Zr}_{0.2}\text{Ti}_{0.8})\text{O}_3$ - $0.5(\text{Ba}_{0.7}\text{Ca}_{0.3})\text{TiO}_3$ ceramic, *J. Appl. Phys.* 113 (2013) (214107-214107-6).
- R. Desfeux, C. Legrand, A. Da Costa, D. Chateigner, R. Bouregba, G. Poullain, Correlation between local hysteresis and crystallite orientation in PZT thin films deposited on Si and MgO substrates, *Surf. Sci.* 600 (2006) 219–228.
- E. Strelcov, Y. Kim, J.C. Yang, Y.H. Chu, P. Yu, X. Lu, S. Jesse, S.V. Kalinin, Role of measurement voltage on hysteresis loop shape in piezoresponse force microscopy, *Appl. Phys. Lett.* 101 (2012) (192902-192902-4).
- D.T. Le, S.J. Kwon, N.R. Yeom, Y.J. Lee, Y.H. Jeong, M.P. Chun, J.H. Nam, J.H. Paik, B.I. Kim, J.H. Cho, Effects of the domain size on local d_{33} in tetragonal $(\text{Na}_{0.53}\text{K}_{0.45}\text{Li}_{0.02})(\text{Nb}_{0.8}\text{Ta}_{0.2})\text{O}_3$ ceramics, *J. Am. Ceram. Soc.* 96 (2013) 174–178.
- D. Maurya, Y. Zhou, B. Chen, M.G. Kang, P. Nguyen, M.K. Hudait, S. Priya, Functionally graded interfaces: role and origin of internal electric field and modulated electrical response, *Appl. Mater. Interfaces* 7 (2015) 22458–22468.